

## Farnesyltransferase pharmacophore model derived from diverse classes of inhibitors

Aijun Lu,<sup>a,b</sup> Jian Zhang,<sup>b</sup> Xiaojin Yin,<sup>a</sup> Xiaomin Luo<sup>b</sup> and Hualiang Jiang<sup>b,c,\*</sup>

<sup>a</sup>JiangSu Simcere Pharmaceutical Research Company Ltd. 210042 Nanjing, China

<sup>b</sup>Center for Drug Discovery and Design, State Key Laboratory of Drug Research, Shanghai Institute of Materia Medica, Shanghai Institutes for Biological Sciences, Chinese Academy of Sciences, 555 Zuchongzhi Road, Shanghai 201203, China

<sup>c</sup>School of Pharmacy, East China University of Science and Technology, Shanghai 200237, China

Received 26 June 2006; revised 3 September 2006; accepted 19 September 2006

Available online 17 October 2006

**Abstract**—A three-dimensional pharmacophore model was developed based on 25 currently available inhibitors, which were carefully selected with great diversity in both molecular structure and bioactivity as required by HypoGen program in the Catalyst software, for discovering new farnesyltransferase (FTase) inhibitors. The best hypothesis (Hypo1), consisting of four features, namely, two hydrogen-bond acceptors, one hydrophobic point, and one ring aromatic feature, has a correlation coefficient of 0.949, a root-mean-square deviation of 1.321, and a cost difference of 163.15, suggesting that a highly predictive pharmacophore model was successfully obtained. The application of the model shows great success in predicting the activities of 227 known FTase inhibitors in our test set with a correlation coefficient of 0.776 with a cross-validation of 98% confidence level. Accordingly, our model should be reliable in identifying structurally diverse compounds with desired biological activity.

© 2006 Elsevier Ltd. All rights reserved.

Significant progress in cancer chemotherapy has been made in recent years with the introduction of novel drugs such as taxol. However, the side effects associated with cytotoxic drugs can deprive patients of a good quality of life and result in a poor therapeutic outcome. As a result, considerable research has recently been devoted to the development of non-cytotoxic anticancer therapy.

Interest in protein farnesyltransferase (FTase) as a potential cancer target was initiated by the observation that the protein product of the ras oncogene required farnesylation for biological function.<sup>1,2</sup> So, over the last two decades protein prenylation has been the subject of intense study and has been found to be critical for the function of key ras proteins involved in signal transduction.<sup>3,4</sup> Because ras proteins play a critical role in signal transduction pathways that control cell growth, differentiation, and apoptosis,<sup>1,5</sup> mutants of human ras proteins are found in 20–30% of all human cancers,<sup>6–8</sup> with an

extraordinarily high prevalence in selected cancer tissues such as pancreatic (90%), colorectal (50%), and lung (40%).<sup>9</sup> Posttranslational modification of proteins by prenylation is an essential step for biological function of ras proteins. Both the regulated and unregulated oncogenic transforming activities of ras require its physical association with the proximal side of the plasma membrane.<sup>10</sup> So prenylation is a form of lipid modification in which either a C-15 farnesyl or C-20 geranylgeranyl group is covalently attached via a thioether linkage to the cysteine residue of proteins near the carboxyl terminus. This posttranslational modification is catalyzed by FTase. FTase inhibitors (FTIs) block incorporation of farnesyl diphosphate (FPP) into ras and cause reversion of ras transformed cells.<sup>11</sup> Indeed, FTIs have been shown to inhibit the growth of a variety of human tumor lines in cell culture and, more recently, to have clinical efficacy for the treatment of several cancers.<sup>12</sup>

As a number of groups have been pursuing FTIs, a wide range of structural classes have been identified and showed to be somewhat effective in inhibiting FTase activity in human.<sup>13–28</sup> These inhibitors in different classes possess different scaffolds. Thus, quantitative structure–activity relationship (QSAR) for different classes

**Keywords:** Farnesyltransferase; Inhibitor; Anticancer; Pharmacophore model; QSAR.

\* Corresponding author. Tel.: +86 21 50807188; fax: +86 21 50807088; e-mail: [hlijiang@mail.shcnc.ac.cn](mailto:hlijiang@mail.shcnc.ac.cn)

of inhibitors could be useful in digging out valuable information for developing new potent FTase inhibitors. It is widely accepted that pharmacophore model is a well-behaved approach to quantitatively explore common chemical characteristics among a considerable number of structures with great diversity, and qualified pharmacophore model could also be used as a query for searching chemical databases to find new chemical entities. Kaminski and his colleague developed a pharmacophore model by 35 FTase inhibitors, but only with training set and without statistical validation.<sup>24</sup> FTase has being a promising anticancer target, therefore, new information about structure–activity relationship based on more compounds with greater diversity in their structures and activities should be helpful in discovering new FTase inhibitors. In this study, we present a hypothetical image of the primary pharmacophore features responsible for the bioactivity of different classes of FTase inhibitors using the Catalyst software,<sup>29–31</sup> with aims to understand the inhibitory mode of various classes of FTase inhibitors and to discover new anticancer drug leads.

**Materials.** A set of 252 different compounds has been collected from different references,<sup>13–26,28</sup> which involves most class of FTase inhibitors. The datasets are divided into a training set and a test set. We selected 25 compounds as training set with the following rules: (a) Both training and test sets should have structure from similar class of compounds and cover the classes as wide as possible to ensure structural diversity; (b) Both training and test sets should cover the molecular bioactivities (IC<sub>50</sub>) as wide as possible; (c) The most active compounds should be included because they provide critical information on pharmacophore requirements. The training set consists of 25 compounds with significant structural diversity and wide coverage of molecular bioactivities in terms of IC<sub>50</sub> ranging from 0.06 nM to 724 μM (Fig. 1 and Table 2). To validate our pharmacophore hypothesis, 227 compounds with available IC<sub>50</sub> values were used as a test set (Table S1 and Figure S1).

The compounds were built using Catalyst 2D–3D sketcher,<sup>29</sup> and a family of representative conformations was generated for each compound using the best conformational analysis method with Poling algorithm<sup>32</sup> and CHARMM force field parameters.<sup>33</sup> A maximum number of 250 conformations of each compound were selected using ‘best conformer generation’ option with a constraint of 20 kcal/mol energy thresholds above the minimum conformer searched to ensure maximum coverage of the conformational space.

**Pharmacophore generation.** Based on the conformations for each compound, Catalyst4.10 software package<sup>29</sup> was employed to construct possible pharmacophore models. Hypothesis generation in Catalyst has three steps, which is constructive phase, subtractive phase, and optimization phase, respectively. Catalyst identifies actives in constructive phase, while it identifies inactives in subtractive phase. Then in optimization phase, Catalyst attempts to minimize a cost function consisting of two terms. One penalizes the deviation between the

estimated activities of the training set molecules and their experimental values; the other penalizes the complexity of the hypothesis. The generation process stops when the optimization no longer improves the score. Uncertainty influences the first step, called the constructive phase, in the hypothesis generating process.<sup>34</sup> The default uncertainty value of 3 was used for the compound activity, representing the ratio of the uncertainty range of measured biological activity against the actual activity for each compound. Analysis of functional groups on each compound in the training set and try and error revealed that three chemical features, viz., hydrogen-bond acceptors (HA), hydrophobic group (HY), and ring aromatic group (RA), could effectively map all of the critical chemical features. Hence, the three features were selected to form the essential information in this hypothesis generation process.

**HypoGen mode.** Pharmacophores were computed by HypoGen encoded in Catalyst4.10<sup>29</sup> and top 10 hypotheses (Table 1) were exported finally. Most hypotheses have high correlation (>0.9). Interestingly, all but one share same four features: two hydrogen-bond acceptors, one hydrophobic point, and one ring aromatic feature (Fig. 2), which shows the stability of the hypotheses, in other words, reliability. On the basis of the very similar composition of the 10 hypotheses, hypothesis 1 (Hypo1), characterized by the best statistical parameters (Table 1) in terms of its predictive ability, as indicated by the highest correlation coefficient and lowest RMS deviations, has been chosen to represent ‘the pharmacophore model’. Remarkably, the three highest active compounds (compounds 8, 9, and 2 in Table 2) can be nicely mapped onto the Hypo1 model by the best fit values, which are shown in Figures 3A–C, indicating that the Hypo1 model provides reasonable pharmacophoric characteristics of the FTase inhibitors for components of their activities.

**Cost analysis.** In addition to generating a hypothesis, Catalyst also provides two theoretical costs (represented in bit units) to help assess the validity of the hypothesis. The first is the cost of an ideal hypothesis (fixed cost), which represents the simplest model that fits all data perfectly. The second is the cost of the null hypothesis (null cost), which represents the highest cost of a pharmacophore with no features and which estimates activity to be the average of the activity data of the training set molecules. They represent the upper and lower bounds for the hypotheses that are generated. A generated hypothesis with a score that is substantially below that of the null hypothesis is likely to be statistically significant and bears visual inspection. The greater the difference between the cost of the generated hypothesis and the cost of the null hypothesis, the less likely it is that the hypothesis reflects a chance correlation. A value of 40–60 bits between them for a pharmacophore hypothesis may indicate that it has 75–90% probability of correlating the data. The total fixed cost of the run is 101.34, the cost of the null hypothesis is 294.92, and the total cost of the Hypo1 is 131.77 (Table 1). Then, the cost range between Hypo1 and the fixed cost is 30.43, while that between the null hypothesis and Hypo1 is 163.15 (Table 1),

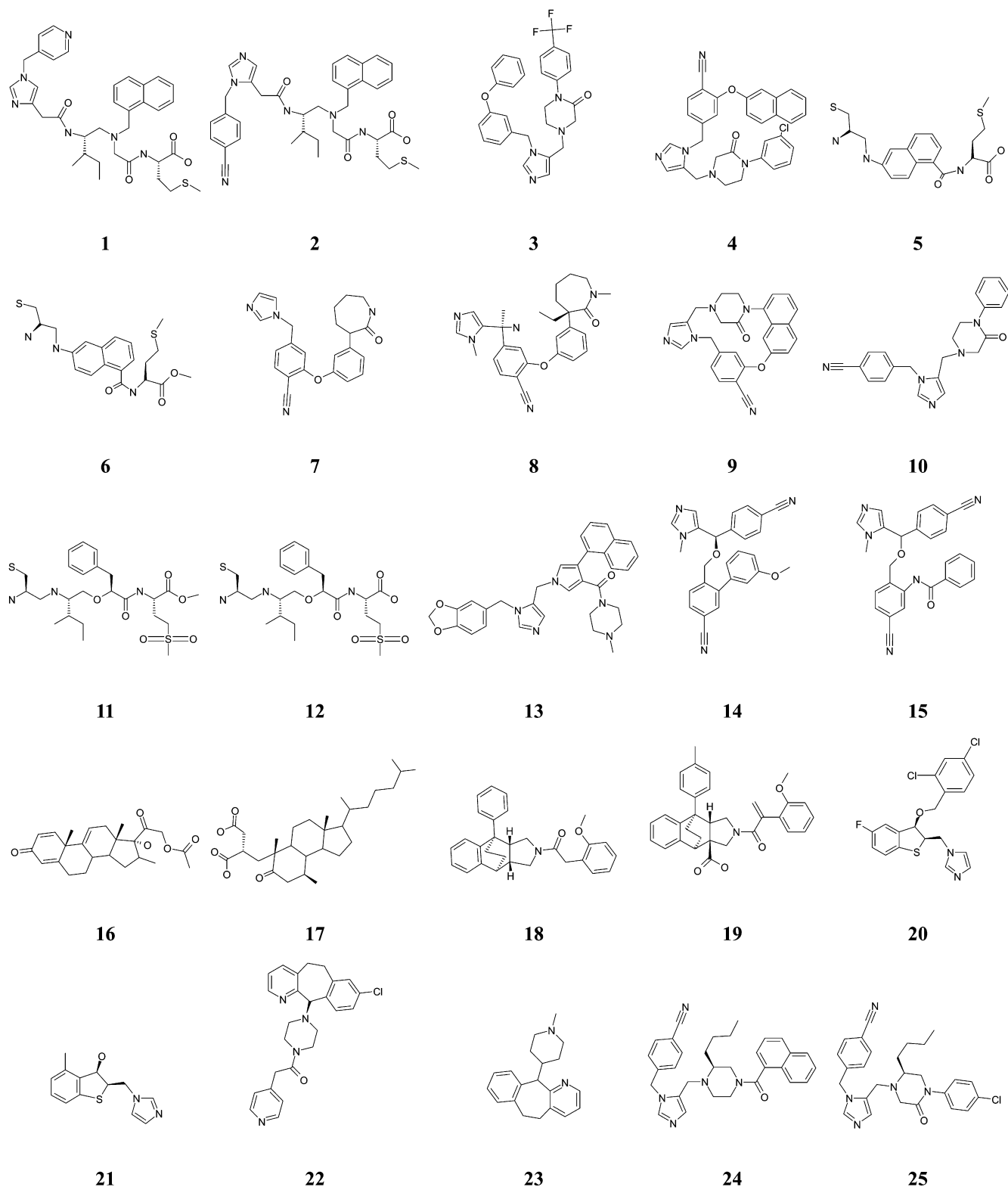


**Figure 1.** Chemical structures of the 25 training set molecules applied to HypoGen pharmacophore generation.

which shows that Hypo1 has more than 90% probability of correlating the data. Noticeably, the total cost of Hypo1 was much closer to the fixed cost than to the null cost. Furthermore, a high correlation coefficient of 0.949 was observed with RMS value of 1.321 and the configuration cost of 16.12, demonstrating that we have

successfully developed a reliable pharmacophore model with high predictivity.

*Score hypothesis.* To verify Hypo1's discriminability among FTase inhibitors with different order of magnitude activity, all training set compounds were classified

**Table 1.** Results of top 10 pharmacophore hypotheses generated using training set

Hypothesis	Total cost	Cost difference <sup>a</sup>	RMS <sup>b</sup>	Correlation ( <i>r</i> )	Features <sup>c</sup>
1	131.77	163.15	1.321	0.949	HA, HA, HY, RA
2	146.56	148.36	1.737	0.908	HA, HA, HY, RA
3	146.87	148.05	1.629	0.922	HA, HA, HY, RA
4	147.71	147.21	1.721	0.910	HA, HA, HY, RA
5	150.73	144.19	1.825	0.898	HA, HA, HY, RA
6	150.96	143.96	1.800	0.901	HA, HA, HY, RA
7	151.9	143.02	1.798	0.902	HA, HA, HY, RA
8	156.02	138.90	1.929	0.885	HA, HA, HY, RA
9	156.03	138.89	1.995	0.875	HA, HA, HY, RA
10	161.83	133.09	2.090	0.862	HA, HY, HY, RA

<sup>a</sup> Cost difference = null cost – total cost. Null cost = 294.92. Fixed cost = 101.34. Configuration cost = 16.12. All cost units are in bits. Configuration cost: a fixed cost which depends on the complexity of the hypothesis space being optimized.

<sup>b</sup> RMS, the deviation of the log (estimated activities) from the log (measured activities) normalized by the log (uncertainties).

<sup>c</sup> HA, hydrogen-bond acceptor; HY, hydrophobic feature; RA, ring aromatic feature.

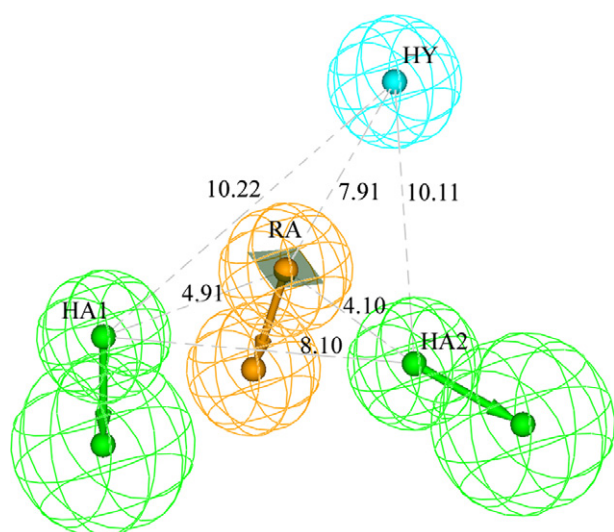


**Figure 2.** The best hypothesis model Hypo1 produced by the Hypo-Gen module in Catalyst 4.10 software package. Pharmacophore features are color-coded with light-blue for hydrophobic groups, orange for ring aromatic group, and green for hydrogen-bond acceptor. Distance between pharmacophore features is reported in angstroms. HY, hydrophobic group; HA1, hydrogen-bond acceptor 1; HA2, hydrogen-bond acceptor 2; RA, ring aromatic group.

by their activity as highly active ( $\leq 100$  nM, +++), moderately active (100–10,000 nM, ++), and inactive ( $>10,000$  nM, +). The actual and estimated FTase inhibitor activities of the 25 compounds based on Hypo1 are listed in Table 2. All the compounds except compounds **1**, **6**, **11**, and **20** were classified correctly (Table 2). The discrepancy between the actual and estimated activity observed for the four compounds was only about 1 order of magnitude, which might be an artifact of the program that uses different number of degrees of freedom for these compounds to mismatch the pharmacophore model. The error factor is also reported in Table 2. It shows that 23 molecules out of the 25 molecules in the training set have errors less than 10 which means that the activity prediction of these compounds falls between 10-fold greater and 1/10 of the actual activity, while the remaining two have errors not higher than 16. For compound **3**, the phenyl was mapped into HY feature. However, additional trifluoromethyl connecting the phenyl

may slightly conflict with FTase, which cannot be detected in Hypo1 generated by HypoGen module. Therefore, overestimated value on activity in the compound **12** is so flexible that it is hard to find true active conformation in prediction, which may be the reason for its underestimated value. The results confirm that our hypothesis is a reliable model for describing the SAR in the training set. In the study, all but one highly active compounds map the first hydrogen-bond acceptor feature (HA1), and two least active inhibitors do not have this feature. Furthermore, HA1 maps on the sulfhydryl which is a key group for bioactivity in peptide-like inhibitor or nitrogen atom of imidazole (Fig. 3) which also plays an important role in the bioactivity discussed by many other researchers.<sup>13,28</sup> Also, lots of compounds containing imidazole designed for inhibiting FTase show very potent activities.<sup>13,16,17,21,25</sup> Combining the previous reports and results described in the study, it seems that this feature should be mainly responsible for the high molecular bioactivity, thus, should be taken into account in discovering or designing novel FTase inhibitors.

*Validation of the constructed pharmacophore model.* The actual activity versus estimated activity of the 227 compounds in the test is shown in Table S1 in the Supporting Information. A correlation coefficient of 0.776 generated using the test set compounds shows a good correlation between the actual and estimated activities. Detailedly, 92 of 109 highly actives (84%), 63 of 77 moderately active (82%), and 13 of 41 inactive compounds (32%) were predicted correctly. Seventeen highly active compounds were underestimated as moderately active; seven moderately active compounds were underestimated as inactive and other seven moderately active compounds were overestimated as highly active; most of inactive compounds were overestimated as moderately active. In conclusion, most of the compounds in the test set were predicted correctly, but many inactive compounds in the test set were predicted overestimated, which mean the hypothesis is suited for screening high active compounds.

The mapping of test compound **65** on Hypo1, which is the azepinone ring R-stereoisomer of compound **8**, is

**Table 2.** Output of the score hypothesis process on the training set

Compound (Ref.)	True IC <sub>50</sub> (nM)	Estimated IC <sub>50</sub> (nM)	Error factor <sup>a</sup>	Fit value <sup>b</sup>	Activity scale <sup>c</sup>	Estimated activity scale	Mapped features			
							HA1	HA2	HY	RA
1 (13)	74	210	+2.9	8.58	+++	++	+	+	+	-
2 (13)	0.15	0.36	+2.4	11.35	+++	+++	+	+	+	+
3 (14)	5800	420	-14	8.28	++	++	+	+	+	-
4 (14)	1	0.61	-1.6	11.12	+++	+++	+	+	+	+
5 (15)	18	17	-1	9.67	+++	+++	+	-	+	+
6 (15)	500	83	-6	8.99	++	+++	+	-	+	+
7 (16)	41	30	-1.4	9.43	+++	+++	-	+	+	+
8 (16)	0.06	0.018	-3.3	12.65	+++	+++	+	+	+	+
9 (17)	0.1	0.81	+8.1	11	+++	+++	+	+	+	+
10 (18)	5	6.2	+1.2	10.11	+++	+++	+	+	+	+
11 (19)	240	100	-2.3	8.89	++	+++	+	-	+	+
12 (19)	1.8	29	+16	9.45	+++	+++	+	+	+	-
13 (20)	2.4	17	+7	9.68	+++	+++	+	+	+	+
14 (21)	0.35	0.46	+1.3	11.25	+++	+++	+	+	+	+
15 (21)	5	7.9	+1.6	10.01	+++	+++	+	+	+	+
16 (22)	40000	25000	-1.6	6.51	+	+	+	-	+	-
17 (22)	40	99	+2.5	8.91	+++	+++	+	+	+	-
18 (23)	40000	7800	-5.2	7.02	+	+	+	-	+	+
19 (23)	8	37	+4.7	9.34	+++	+++	+	-	+	+
20 (24)	700	94	-7.4	8.93	++	+++	+	-	+	+
21 (24)	270000	31000	-8.5	6.41	+	+	-	+	-	+
22 (24)	140	840	+6	7.98	++	++	-	+	+	-
23 (24)	720000	1.20E+06	+1.7	4.82	+	+	-	-	+	+
24 (25)	21	3.5	-5.9	10.36	+++	+++	+	+	+	+
25 (25)	0.44	1	+2.3	10.9	+++	+++	+	+	+	+

<sup>a</sup> The error factor is computed as the ratio of the measured activity to the activity estimated by the hypothesis or the inverse if estimated is greater than measured.

<sup>b</sup> Fit value indicates how well the features in the pharmacophore overlap the chemical features in the molecule.

<sup>c</sup> Activity scale: +++, IC<sub>50</sub> ≤ 100 nM (highly active); ++, 10,000 nM > IC<sub>50</sub> > 100 nM (moderately active); +, IC<sub>50</sub> ≥ 10,000 nM (inactive).

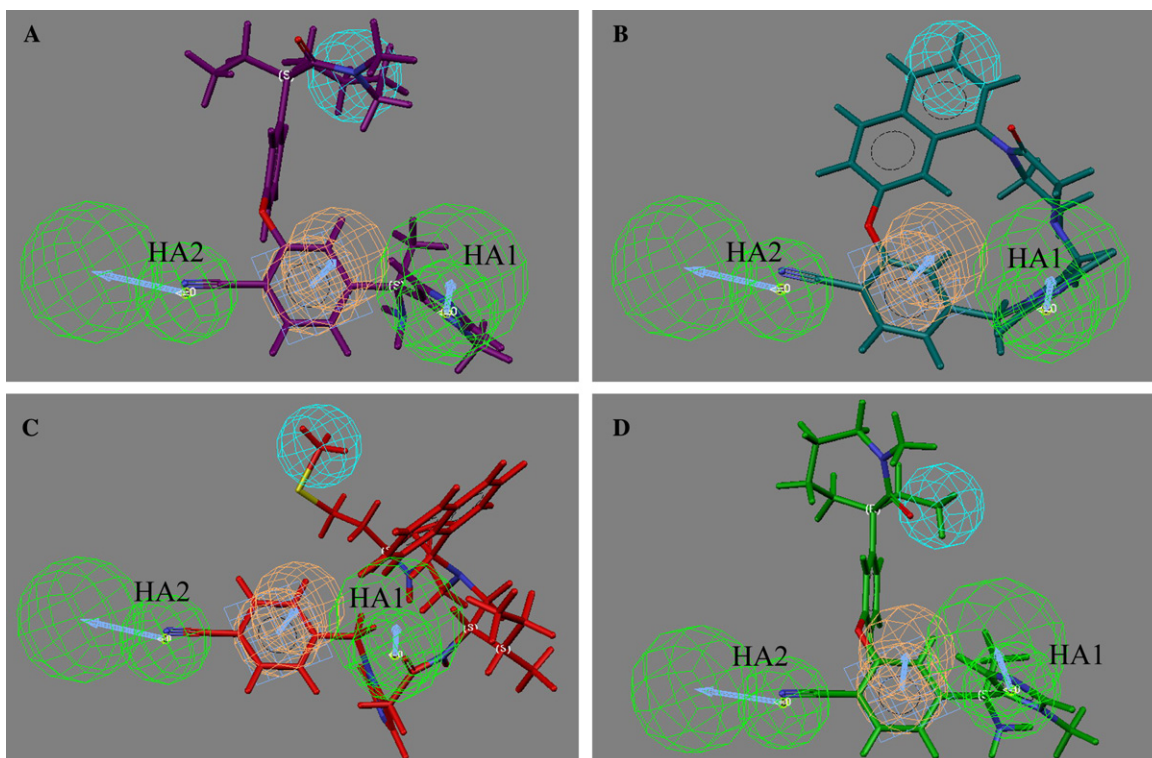


**Figure 3.** Mapping of the three most highly active compounds in training set and one compound in test set on the best hypothesis model Hypo1 (A) compound 8; (B) compound 9; (C) compound 2; (D) compound 65. Pharmacophore features are color-coded with the same as Fig. 2.

**Table 3.** Output parameters of the 10 lowest cost hypotheses resulting from the statistical evaluation procedure according to the Fischer Method

Hypothesis	Total cost	RMS	Correlation
1	178.04	2.252	0.840
2	179.51	2.283	0.836
3	191.08	2.454	0.809
4	193.62	2.215	0.866
5	194.61	2.620	0.776
6	203.42	2.736	0.750
7	205.35	2.754	0.746
8	209.37	2.833	0.727
9	212.31	2.818	0.733
10	212.68	2.849	0.729
Hypo1	131.77	1.321	0.949

shown in Figure 3D. The potency of **8**,  $IC_{50} = 0.06$  nM, is greater than the FTase inhibitory potency of compound **65**,  $IC_{50} = 1.5$  nM. Also, the observation that the azepinone ring of S enantiomer is fitting better on HY can also be derived from the two compounds' mapping on Hypo1.

**Fisher test.** To further evaluate the statistical relevance of the model, the Fischer method<sup>35</sup> was applied. With the aid of the CatScramble program, the experimental activities in the training set were scrambled randomly, and the resulting training set was used for a HypoGen run. All parameters were adopted from the initial HypoGen calculation. This procedure was reiterated 49 times. None of the outcome hypotheses has lower cost score than the initial hypothesis. Table 3 lists the 10 lowest total cost values of the resulting 49 hypotheses. Accordingly, this result indicates that there is a 98% chance for the best hypothesis to represent a true correlation in the training set activity data.<sup>29,30,36,37</sup> Furthermore, all the top 10 hypotheses exported by HypoGen pass 98% Fisher test, which indicates that the models are not random, but meaningful and successful.

For discovering potent FTase inhibitors as new anticancer drug, a ligand-based computational approach was employed to identify molecular structure requirements for active inhibitors. A highly predictive pharmacophore model was generated based on 25 training set compounds by the HypoGen module of Catalyst software package,<sup>29</sup> which consists of two hydrogen-bond acceptors, one hydrophobic point, and one ring aromatic feature. The utility of our pharmacophore model on 227 test set compounds showed that the model is able to accurately differentiate various classes of FTase inhibitors. Thus, the pharmacophore model that we developed should be helpful in identifying novel lead compounds with improved inhibitory activity through 3D database searches, and useful to designing novel FTase inhibitors.

### Supplementary data

Supplementary data associated with this article can be found in the online version at doi:10.1016/j.bmcl.2006.09.055.

### References and notes

- Casey, P. J.; Solski, P. A.; Der, C. J.; Buss, J. E. *Proc. Natl. Acad. Sci. U.S.A.* **1989**, *86*, 8323.
- Willumsen, B. M.; Norris, K.; Papageorge, A. G.; Hubbert, N. L.; Lowy, D. R. *EMBO J.* **1984**, *3*, 2581.
- Casey, P. J.; Seabra, M. C. *J. Biol. Chem.* **1996**, *271*, 5289.
- Marshall, C. J. *Science* **1993**, *259*, 1865.
- Powers, S.; Michaelis, S.; Broek, D.; Santa Anna, S.; Field, J.; Herskowitz, I.; Wigler, M. *Cell* **1986**, *47*, 413.
- Barbacid, M. *Annu. Rev. Biochem.* **1987**, *56*, 779.
- Bos, J. L. *Cancer Res.* **1989**, *49*, 4682.
- Keely, P.; Parise, L.; Juliano, R. *Trends Cell Biol.* **1998**, *8*, 101.
- Cox, A. D.; Der, C. J. *Biochim. Biophys. Acta* **1997**, *1333*, F51.
- Willumsen, B. M.; Christensen, A.; Hubbert, N. L.; Papageorge, A. G.; Lowy, D. R. *Nature* **1984**, *310*, 583.
- James, G. L.; Goldstein, J. L.; Brown, M. S.; Rawson, T. E.; Somers, T. C.; McDowell, R. S.; Crowley, C. W.; Lucas, B. K.; Levinson, A. D.; Marsters, J. C., Jr. *Science* **1993**, *260*, 1937.
- Bell, I. M. *Exp. Opin. Ther. Patents* **2000**, *10*, 1813.
- Anthony, N. J.; Gomez, R. P.; Schaber, M. D.; Mosser, S. D.; Hamilton, K. A.; O'Neil, T. J.; Koblan, K. S.; Graham, S. L.; Hartman, G. D.; Shah, D.; Rands, E.; Kohl, N. E.; Gibbs, J. B.; Oliff, A. I. *J. Med. Chem.* **1999**, *42*, 3356.
- Bergman, J. M.; Abrams, M. T.; Davide, J. P.; Greenberg, I. B.; Robinson, R. G.; Buser, C. A.; Huber, H. E.; Koblan, K. S.; Kohl, N. E.; Lobell, R. B.; Graham, S. L.; Hartman, G. D.; Williams, T. M.; Dinsmore, C. J. *Bioorg. Med. Chem. Lett.* **2001**, *11*, 1411.
- Burns, C. J.; Guitton, J. D.; Baudoin, B.; Lelievre, Y.; Duchesne, M.; Parker, F.; Fromage, N.; Commercon, A. *J. Med. Chem.* **1997**, *40*, 1763.
- deSolms, S. J.; Ciccarone, T. M.; MacTough, S. C.; Shaw, A. W.; Buser, C. A.; Ellis-Hutchings, M.; Fernandes, C.; Hamilton, K. A.; Huber, H. E.; Kohl, N. E.; Lobell, R. B.; Roberson, R. G.; Tsou, N. N.; Walsh, E. S.; Graham, S. L.; Beese, L. S.; Taylor, J. S. *J. Med. Chem.* **2003**, *46*, 2973.
- Dinsmore, C. J.; Bogusky, M. J.; Culbertson, J. C.; Bergman, J. M.; Homnick, C. F.; Zartman, C. B.; Mosser, S. D.; Schaber, M. D.; Roberson, R. G.; Koblan, K. S.; Huber, H. E.; Graham, S. L.; Hartman, G. D.; Huff, J. R.; Williams, T. M. *J. Am. Chem. Soc.* **2001**, *123*, 2107.
- Dinsmore, C. J.; Bergman, J. M.; Wei, D. D.; Zartman, C. B.; Davide, J. P.; Greenberg, I. B.; Liu, D.; O'Neill, T. J.; Gibbs, J. B.; Koblan, K. S.; Kohl, N. E.; Lobell, R. B.; Chen, I. W.; McLoughlin, D. A.; Olah, T. V.; Graham, S. L.; Hartman, G. D.; Williams, T. M. *Bioorg. Med. Chem. Lett.* **2001**, *11*, 537.
- Kohl, N. E.; Wilson, F. R.; Mosser, S. D.; Giuliani, E.; deSolms, S. J.; Conner, M. W.; Anthony, N. J.; Holtz, W. J.; Gomez, R. P.; Lee, T. J., et al. *Proc. Natl. Acad. Sci. U.S.A.* **1994**, *91*, 9141.
- Lee, H.; Lee, J.; Lee, S.; Shin, Y.; Jung, W.; Kim, J. H.; Park, K.; Kim, K.; Cho, H. S.; Ro, S.; Lee, S.; Jeong, S. W.; Choi, T.; Chung, H. H.; Koh, J. S. *Bioorg. Med. Chem. Lett.* **2001**, *11*, 3069.
- Wang, L.; Wang, G. T.; Wang, X.; Tong, Y.; Sullivan, G.; Park, D.; Leonard, N. M.; Li, Q.; Cohen, J.; Gu, W. Z.; Zhang, H.; Bauch, J. L.; Jakob, C. G.; Hutchins, C. W.; Stoll, V. S.; Marsh, K.; Rosenberg, S. H.; Sham, H. L.; Lin, N. H. *J. Med. Chem.* **2004**, *47*, 612.
- Lingham, R. B.; Silverman, K. C.; Jayasuriya, H.; Kim, B. M.; Amo, S. E.; Wilson, F. R.; Rew, D. J.; Schaber, M.

- D.; Bergstrom, J. D.; Koblan, K. S.; Graham, S. L.; Kohl, N. E.; Gibbs, J. B.; Singh, S. B. *J. Med. Chem.* **1998**, *41*, 4492.
23. Giraud, E.; Luttmann, C.; Lavelle, F.; Riou, J. F.; Mailliet, P.; Laoui, A. *J. Med. Chem.* **2000**, *43*, 1807.
24. Kaminski, J. J.; Rane, D. F.; Snow, M. E.; Weber, L.; Rothofsky, M. L.; Anderson, S. D.; Lin, S. L. *J. Med. Chem.* **1997**, *40*, 4103.
25. Williams, T. M.; Bergman, J. M.; Brashear, K.; Breslin, M. J.; Dinsmore, C. J.; Hutchinson, J. H.; MacTough, S. C.; Stump, C. A.; Wei, D. D.; Zartman, C. B.; Bogusky, M. J.; Culberson, J. C.; Buser-Doepner, C.; Davide, J.; Greenberg, I. B.; Hamilton, K. A.; Koblan, K. S.; Kohl, N. E.; Liu, D.; Lobell, R. B.; Mosser, S. D.; O'Neill, T. J.; Rands, E.; Schaber, M. D.; Huff, J. R., et al. *J. Med. Chem.* **1999**, *42*, 3779.
26. Gibbs, J. B.; Pompliano, D. L.; Mosser, S. D.; Rands, E.; Lingham, R. B.; Singh, S. B.; Scolnick, E. M.; Kohl, N. E.; Oliff, A. *J. Biol. Chem.* **1993**, *268*, 7617.
27. Leonard, D. M. *J. Med. Chem.* **1997**, *40*, 2971.
28. Leonard, D. M.; Shuler, K. R.; Poulter, C. J.; Eaton, S. R.; Sawyer, T. K.; Hodges, J. C.; Su, T. Z.; Scholten, J. D.; Gowan, R. C.; Sebolt-Leopold, J. S.; Doherty, A. M. *J. Med. Chem.* **1997**, *40*, 192.
29. CATALYST 4.10. Accelrys, Inc., San Diego, CA, 2005, <http://www.accelrys.com>.
30. Funk, O. F.; Kettmann, V.; Drimal, J.; Langer, T. *J. Med. Chem.* **2004**, *47*, 2750.
31. Kurogi, Y.; Guner, O. F. *Curr. Med. Chem.* **2001**, *8*, 1035.
32. Smellie, A.; Teig, S.; Towbin, P. *J. Comput. Chem.* **1994**, *16*, 171.
33. Brooks, B. R.; Bruccoleri, R. E.; Olafson, B. D.; States, D. J.; Swaminathan, S.; Karplus, M. J. *J. Comput. Chem.* **1983**, *4*, 187.
34. Güner, O. F. In *Pharmacophore Perception, Development, and Use in Drug Design*; International University Line: La Jolla, California, 2000, pp 173.
35. Fischer, R. In *The Principle of Experimentation, Illustrated by a Psycho-Physical Experiment. The Design of Experiments*, 8th ed.; Hafner Publishing Co.: New York, 1966, pp chapter II.
36. Krovat, E. M.; Langer, T. *J. Med. Chem.* **2003**, *46*, 716.
37. Tafi, A.; Costi, R.; Botta, M.; Di Santo, R.; Corelli, F.; Massa, S.; Ciacci, A.; Manetti, F.; Artico, M. *J. Med. Chem.* **2002**, *45*, 2720.